Atmos. Chem. Phys. Discuss., doi:10.5194/acp-2016-484, 2016
Manuscript under review for journal Atmos. Chem. Phys.
Published: 22 June 2016


Atmospheric Chemistry and Physics Discussions

# Detection of atmospheric gaseous amines and amides by a high resolution time-of-flight chemical ionization mass spectrometer with protonated ethanol reagent ions

Lei Yao[1], Ming-Yi Wang[1], Xin-Ke Wang[1], Yi-Jun Liu[1,2], Hang-Fei Chen[1], Jun Zheng[3], Wei Nie[4,5], Ai-Jun Ding[4,5], Fu-Hai Geng[6], Dong-Fang Wang[7], Jian-Min Chen[1], Douglas R. Worsnop[8], Lin Wang[1,5]*

[1] *Shanghai Key Laboratory of Atmospheric Particle Pollution and Prevention (LAP[3]), Department of Environmental Science & Engineering, Fudan University, Shanghai 200433, China*

[2] *now at Pratt school of engineering, Duke University, Durham, NC 27705,USA*

[3] *Jiangsu Key Laboratory of Atmospheric Environment Monitoring and Pollution Control, Nanjing University of Information Science & Technology, Nanjing 210044, China*

[4] *Joint International Research Laboratory of Atmospheric and Earth System Sciences, School of Atmospheric Science, Nanjing University, 210023, Nanjing, China*

[5] *Collaborative Innovation Center of Climate Change, Nanjing, Jiangsu Province, China*

[6] *Shanghai Meteorology Bureau, Shanghai 200135, China*

[7] *Shanghai Environmental Monitoring Center, Shanghai 200030, China*

[8] *Aerodyne Research, Billerica, MA 01821, USA*

* *Corresponding Author: L.W., email, lin_wang@fudan.edu.cn; phone, +86-21-65643568; fax, +86-21-65642080.*

Atmos. Chem. Phys. Discuss., doi:10.5194/acp-2016-484, 2016
Manuscript under review for journal Atmos. Chem. Phys.
Published: 22 June 2016


Atmospheric Chemistry and Physics Discussions


## Abstract

Amines and amides are important atmospheric organic-nitrogen compounds but high time resolution, highly sensitive, and simultaneous ambient measurements of these species are rather sparse. Here, we present the development of a high resolution time-of-flight chemical ionization mass spectrometer (HR-ToF-CIMS) method utilizing protonated ethanol as reagent ions to simultaneously detect atmospheric gaseous amines ($C_1$ to $C_6$) and amides ($C_1$ to $C_6$). This method possesses sensitivities of 5.6-19.4 Hz $pptv^{-1}$ for amines and 3.8-38.0 Hz $pptv^{-1}$ for amides under total reagent ion signals of ~0.32 MHz, and detection limits of 0.10-0.50 pptv for amines and 0.29-1.95 pptv for amides at 3σ of the background signal for a 1-min integration time, respectively. Controlled characterization in the laboratory indicates that relative humidity has significant influences on detection of amines and amides, whereas the presence of organics has no obvious effects. Ambient measurements of amines and amides utilizing this method were conducted from 25 July 2015 to 25 August 2015 in urban Shanghai, China. While the concentrations of amines ranged from a few pptv to hundreds of pptv, concentrations of amides varied from tens of pptv to a few ppbv. Among the $C_1$- to $C_6$-amines, the $C_2$-amines were the dominant species with concentrations up to 130 pptv. For amides, the $C_3$-amides (up to 8.7 ppb) were the most abundant species. The diurnal profiles of amines and amides suggest that in addition to the secondary formation of amides in the atmosphere, industrial emissions could be important sources of amides in urban Shanghai. During the campaign, photo-oxidation of amines and amides might be a main loss pathway for them in day time, and wet deposition was also an important sink.

Atmos. Chem. Phys. Discuss., doi:10.5194/acp-2016-484, 2016
Manuscript under review for journal Atmos. Chem. Phys.
Published: 22 June 2016


Atmospheric Chemistry and Physics Discussions

## 1 Introduction

Amines and amides are nitrogen-containing organic compounds widely observed in the atmosphere (Ge et al., 2011). They are emitted from a variety of natural and anthropogenic sources including agriculture, biomass burning, animal husbandry, cooking, synthetic leather, carbon capture, and other industrial processes (Finlayson-Pitts and Pitts, 2000; Ge et al., 2011; Kim et al., 2004; Kuhn et al., 2011; Nielsen et al., 2012; Zhu et al., 2013). In addition to the primary sources, amides can be formed from the degradation processes of amines (Nielsen et al., 2012) and atmospheric accretion reactions of organic acids with amines or ammonia (Barsanti and Pankow, 2006).

Once in the atmosphere, amines and amides can react with atmospheric oxidants (*e.g.*, OH and $NO_3$ radicals, Cl atoms, and $O_3$), and lead to gaseous degradation products and formation of secondary organic aerosols (Barnes et al., 2010; Bunkan et al., 2016; El Dib and Chakir, 2007; Lee and Wexler, 2013; Malloy et al., 2009; Murphy et al., 2007; Nielsen et al., 2012). In addition, the basic nature of amines certainly justifies their participation in atmospheric new particle formation and growth events (Almeida et al., 2013; Erupe et al., 2011; Glasoe et al., 2015; Smith et al., 2010; Yu et al., 2012; Zhang et al., 2012). Heterogeneous uptake of amines by acidic aerosols and displacement reactions of ammonium ions by amines can significantly alter the physio-chemical properties of aerosol particles (Qiu et al., 2011; Wang et al., 2010a; Wang et al., 2010b).

Atmospheric amines have been measured in different surroundings. Kieloaho et al. (2013) used offline acid-impregnated fiberglass filter collection together with analysis by high performance liquid chromatography electrospray ionization ion trap mass spectrometer, and reported that the highest concentrations of $C_2$-amines (ethylamine (EA) + dimethylamine (DMA)) and $C_3$-amines (propylamine (PA) + trimethylamine (TMA)) reached 157±20 pptv (parts per trillion by volume) and 102±61 pptv, respectively, in boreal forests, southern Finland. Using a similar detection method, the mean concentrations of $C_2$-amines (EA+DMA), $C_3$-amines (PA+TMA), butylamine (BA), diethylamine (DEA) and triethylamine (TMA) were measured to be 23.6 pptv, 8.4 pptv, 0.3 pptv, 0.3 pptv, and 0.1 pptv, respectively, in urban air of Helsinki, Finland (Hellén et al., 2014). Detection of gaseous alkyl amines were conducted in Toronto, Canada using an ambient ion monitor ion chromatography system, and the concentrations of DMA, and TMA+DEA were both less than 2.7 ppt (VandenBoer et al. 2011). Recently, online detection of atmospheric amines using chemical ionization mass spectrometer is becoming the trend. Yu and Lee (2012) utilized a quadrupole chemical ionization mass spectrometer

Atmos. Chem. Phys. Discuss., doi:10.5194/acp-2016-484, 2016
Manuscript under review for journal Atmos. Chem. Phys.
Published: 22 June 2016


Atmospheric Chemistry and Physics Discussions

(CIMS) with protonated ethanol and acetone ions as reagent ions to measure $C_2$-amines (8±3 pptv) and $C_3$-amines (16±7 pptv) in Kent, Ohio. A similar method detected a few pptv to tens of pptv $C_3$-amines in Alabama forest (You et al., 2014). Sellegri et al. (2005) reported the mean concentration of TMA and DMA were 59 pptv and 12.2 pptv, respectively, in Hyytiälä forest, with a quadrupole-CIMS with hydronium ions as reagent ions. Measurements of amines in urban areas did not show significant differences in terms of concentration. The average of total amines ($C_1$-$C_3$) was 7.2±7.4 pptv in Nanjing, China, as measured by a high resolution time-of-flight CIMS (HR-ToF-CIMS) with hydronium ions as reagent ions (Zheng et al., 2015). Measurements by an ambient pressure proton transfer mass spectrometer (AmPMS) in urban Atlanta showed that trimethylamine (TMA) (or isomers or amide) was the most abundant amine-species and that the concentration of DMA was ~3 pptv (Hanson et al., 2011).

To the best of our knowledge, gaseous amides were not previously measured in ambient air, except for two studies that briefly described the detection of a few amides near the emission source. Zhu et al. (2013) detected formamide (FA) ($C_1$-amide) formed from degradation of mono-ethanolamine in emissions from an industrial carbon capture facility, using proton transfer reaction time-of-flight mass spectrometry (PTR-ToF-MS). Furthermore, up to 4350 pptv of dimethylamide was observed near a municipal incinerator, waste collection center and sewage treatment plant (Leach et al., 1999).

Given the important role of amines in atmospheric nucleation and other physio-chemical processes, and the potential involvement of amides in a number of atmospheric processes, it is necessary to develop high time resolution and highly sensitive detection techniques for measurements of ambient amines and amides. Previous studies have proven CIMS to be a powerful instrument to detect gaseous amines and amides in laboratory studies and field campaigns (Borduas et al., 2015; Bunkan et al., 2016; Hanson et al., 2011; Sellegri et al., 2005; Yu and Lee, 2012; You et al., 2014; Zheng et al., 2015). However, the detection method for ambient amides with much lower concentrations than those in laboratory studies is still lacking. The popular usage of hydronium ions as reagent ions (*e.g.* PTR-MS and AmPMS) potentially leads to the relative humidity (RH) dependence of the background and ambient amine signals, adding uncertainties to measurement results (Hanson et al., 2011; Zheng et al., 2015; Zhu et al., 2013). In addition, constrained by the mass resolution of the quadrupole-detector mass spectrometer, it is difficult to distinguish protonated

Atmos. Chem. Phys. Discuss., doi:10.5194/acp-2016-484, 2016
Manuscript under review for journal Atmos. Chem. Phys.
Published: 22 June 2016


Atmospheric Chemistry and Physics Discussions

amines and amides with an identical unit mass, which pre-excludes the possibility of simultaneous measurements of amines and amides. For example, the *m/z* (mass to charge ratio) value of protonated trimethylamine ($C_3H_9N{\cdot}H^+$, *m/z* 60.0808) and that of protonated acetamide ($C_2H_5NO{\cdot}H^+$, *m/z* 60.0444) are very close.

In the present study, a HR-ToF-CIMS method utilizing protonated ethanol as reagent ions has been developed to simultaneously detect atmospheric gaseous amines ($C_1$ to $C_6$) and amides ($C_1$ to $C_6$). Protonated ethanol was selected as the reagent ions because the higher proton affinity of ethanol (185.6 kcal $mol^{-1}$) than that of water (165.2 kcal $mol^{-1}$), as shown in Table 1, results in more selectivity for detecting high proton affinity species (*e.g.* > 196 kcal $mol^{-1}$ for amines and amides) (Nowak, 2002; Yu and Lee, 2012; You et al., 2014). The influences of RH and organics on amine and amide detection were characterized in the laboratory. Ambient measurements of amines and amides utilizing this method were performed from 25 July 2015 to 25 August 2015 in urban Shanghai, China. During the campaign, a Filter Inlet for Gases and AEROsols (FIGAERO) was interfaced to HR-ToF-CIMS (Lopez-Hilfiker et al., 2014) but only results on gaseous $C_1$-$C_6$ amines and amides are presented. The potential sources and sinks of amines and amides are discussed.

## 2 Experimental

### 2.1 Instrumentation

An Aerodyne HR-ToF-CIMS (Bertram et al., 2011) with protonated ethanol as reagent ions has been deployed to detect gaseous amines ($C_1$ to $C_6$) and amides ($C_1$ to $C_6$). Protonated ethanol reagent ions were generated by passing a pure air flow of 1 L $min^{-1}$ (liter per minute) supplied by a zero air generator (Aadco 737) through a Pyrex bubbler containing ethanol (≥ 96%, J.T.Baker) and then through a 0.1 mCi $^{241}Am$ radioactive source. A sample flow of 1.35 L $min^{-1}$ was introduced into the ion-molecular reaction (IMR) chamber where the sample flow and the reagent ion flow converge. The pressures of the IMR chamber and the small-segmented quadrupole (SSQ) were regulated at ~100 mbar and ~2.8 mbar, respectively, to increase the instrument sensitivity. Under such conditions, the ion-molecular reaction time was ~320 ms in the IMR. To minimize wall-loss of analytes on the inner surface of IMR, the temperature of IMR was maintained at an elevated temperature (50°C). The data of HR-ToF-CIMS was collected at 1 Hz time resolution.

Under dry conditions, the most abundant reagent ion was protonated ethanol dimer

Atmos. Chem. Phys. Discuss., doi:10.5194/acp-2016-484, 2016
Manuscript under review for journal Atmos. Chem. Phys.
Published: 22 June 2016


Atmospheric Chemistry and Physics Discussions

163 (($(C_2H_5OH)_2 \cdot H^+$, *m/z* 93.0910), with the next dominant ions being protonated ethanol monomer
164 ( $(C_2H_5OH) \cdot H^+$, *m/z* 47.0491) and protonated ethanol trimer (($(C_2H_5OH)_3 \cdot H^+$, *m/z* 139.1329). The
165 presence of water led to formation of clusters of protonated ethanol with water ($C_2H_5OH \cdot H_2O \cdot H^+$) and
166 hydronium ions and their hydrates (($(H_2O)_n \cdot H^+$, n=1, 2 and 3). A typical mass spectrum under < 20%
167 RH is shown in Figure S1. The ratios of oxygen cation ($O_2^+$), the clusters of protonated ethanol with
168 water ($C_2H_5OH \cdot H_2O \cdot H^+$), and hydronium ions (($(H_2O)_n \cdot H^+$, n=1, 2 and 3) to the sum of $(C_2H_5OH) \cdot H^+$,
169 $(C_2H_5OH)_2 \cdot H^+$, and $(C_2H_5OH)_3 \cdot H^+$ were ~0.001, ~0.026, and ~0.011, respectively.

170 Amines and amides reacted dominantly with protonated ethanol ions through proton transfer
171 reactions. The ion-molecular reactions of amines (denoted as $NR_3$, R=H or an alkyl group) and amides
172 (denoted as $R'_2NC(O)R$, R'=H or an alkyl group) with protonated ethanol reagent ions can be showed
173 as the following (You et al., 2014; Yu and Lee, 2012):

174 $(C_2H_5OH)_n \cdot H^+ + NR_3 \longrightarrow (C_2H_5OH)_j \cdot NR_3 \cdot H^+ + (n\text{-}j)C_2H_5OH$ (R1)

175 $(C_2H_5OH)_n \cdot H^+ + R'_2NC(O)R \longrightarrow (C_2H_5OH)_j \cdot R'_2NC(O)R \cdot H^+ + (n\text{-}j)C_2H_5OH$ (R2)

176 where $n$ = 1, 2, and 3, and $j$ = 0 and 1.

177 **2.2 Calibration of amines and amides**

178 Amines and amides were calibrated using permeation sources. Permeation tubes for amines
179 (methylamine (MA), dimethylamine (DMA), trimethylamine (TMA), and diethylamine (DEA)) were
180 purchased from VICI Inc. USA, whereas those for amides (formamide (FA), ≥ 99.5%, GC, Sigma
181 Aldrich; acetamide (AA), ≥ 99%, GC, Sigma Aldrich; and propanamide (PA), ≥ 96.5%, GC, Sigma
182 Aldrich) were home-made using 1/4 inch Teflon tubes with the ends sealed with Teflon blockers. The
183 permeation tube was placed in a U-shape glass tube with a diameter of 2.5 cm that was immersed in a
184 liquid bath with precise temperature regulation (Zheng et al., 2015). A high purity (≥99.999%)
185 nitrogen flow typically at 0.1 L $min^{-1}$ was used as the carrier gas to carry the permeated compounds to
186 HR-ToF-CIMS for detection.

187 The concentration of an amine in the outflow of the permeation tube was referred to that as
188 determined by an acid-base titration method (Freshour et al., 2014). The high purity nitrogen flow
189 containing an amine standard was bubbled through a HCl solution (pH = ~4.5) with a small amount of
190 KCl (~5 mM) added to facilitate measurements of pH values. Reagents HCl (~37 wt% in water) and
191 KCl (≥ 99%) were of ACS reagents and purchased from Sigma Aldrich. The concentration of the

Atmos. Chem. Phys. Discuss., doi:10.5194/acp-2016-484, 2016
Manuscript under review for journal Atmos. Chem. Phys.
Published: 22 June 2016


Atmospheric Chemistry and Physics Discussions

amine was derived according to variations of the pH values with titration time. The pH values were averaged and recorded by a pH meter (340i, WTW, Germany) every 5 min.

In the case of amides, a permeated alkyl-amide was trapped in a $HNO_3$ solution with a pH of ~2.5 that was diluted from reagent $HNO_3$ (~70 wt% in water, ACS reagent, Sigma Aldrich). Hydrolysis of the alkyl-amide occurred under acidic conditions leading to formation of $NH_4^+$ (Cox and Yates, 1981). The concentration of $NH_4^+$ was quantified using Ion Chromatography (Metrohm 833, Switzerland), and the permeation rate of the alkyl-amide was derived from the variation of $NH_4^+$ with the time period of hydrolysis.

The total ethanol reagent ion signals during the laboratory calibration were typically ~0.32 MHz.

### 2.3 Influence of RH and organics

Experiments were performed to characterize the influence of RH and organics on the detection of amines and amides. The schematics of our experimental setup are shown in Figure S2 (A for tests at elevated RH and B for tests in presence of organics), where the tubes and valves are made of polytetrafluoroethylene (PTFE) and perfluoroalkoxy (PFA) materials to minimize absorption of amines/amides on the inner surface of tubes and valves. To examine the influence of RH, a pure air flow was directed through a bubbler filled with 18.2 MΩ·cm deionized water, and then mixed with the amine/amide flow of 0.1 L $min^{-1}$ generated from the permeation sources. The examined RH ranged from 4 % to 65%.

α-pinene, a typical biogenic organic compound, and p-xylene, a typical anthropogenic compound, were chosen to examine the influence of organics on detection of amines and amides. The amines/amide flow was mixed with organics for ~0.2 s before entering the IMR. During the characterization, the air flow (15 L $min^{-1}$) containing α-pinene or p-xylene with concentrations up to hundreds of ppbv (parts per billion by volume) was initially mixed the amine/amide flow of 0.1 L $min^{-1}$ generated from the permeation sources. Then ozone and OH radicals were generated from an $O_2/H_2O$ flow of $2\times10^{-3}$ L $min^{-1}$ by turning on a Hg-lamp (Jelight model 600, USA). Photochemical reactions of α-pinene or p-xylene occurred and a much more complex mixture of organics was subsequently mixed with the amine/amide flow.

### 2.4 Field campaign in urban Shanghai

The ethanol HR-ToF-CIMS was deployed for a field campaign at the Fudan site (31° 17′ 54" N,

Atmos. Chem. Phys. Discuss., doi:10.5194/acp-2016-484, 2016
Manuscript under review for journal Atmos. Chem. Phys.
Published: 22 June 2016


Atmospheric Chemistry and Physics Discussions

121° 30′ 05" E) on the campus of Fudan University from 25 July through 25 August, 2015. This monitoring site is on the rooftop of a teaching building that is ~20 m above ground. About 100 m to the north is the Middle Ring that is one of the main overhead highways in Shanghai. This site is also influenced by local industrial and residential activities. Hence, the Fudan site is a representative urban site (Ma et al., 2014; Wang et al., 2013a; Wang et al., 2016; Xiao et al., 2015).

The schematic of the ethanol HR-ToF-CIMS setup during the field campaign is shown in Figure S3. Ambient air was drawn into a PTFE tubing with a length of 2 m and an inner diameter of 3/8 inch. To minimize the wall-loss of amines and amides, a high sampling flow rate (15 L $min^{-1}$) was adopted, resulting in an inlet residence time of ~0.26 s. Also, the PTFE tubing was heated to 50℃ by heating tapes. Because of the high concentrations of volatile organic compounds in the air of urban Shanghai, reagent ion depletion occurred during the initial tests of measurements of ambient samples. Hence, the ambient air was diluted with a high purity nitrogen flow with a dilution ratio of ~1:4.6. Under such condition, variation of the total reagent ions ($(C_2H_5OH)\cdot H^+$, $(C_2H_5OH)_2\cdot H^+$, and $(C_2H_5OH)_3\cdot H^+$) was less than 10% between measurements of the background air and the ambient sample. The ethanol reagent ion signals were typically around 0.35 MHz throughout the entire campaign. To take the variation in total reagent ions between in laboratory calibration and during field measurements into account, ambient concentrations of amines and amides were calculated according to

$$[\text{amines or amides}]_{\text{ambient}} = C_{\text{amines or amides}} \times \frac{\sum_{n=0-1}(\text{amines or amides})\cdot(C_2H_5OH)_n\cdot H^+}{\sum_{n=1-3}(C_2H_5OH)_n H^+} \quad (1)$$

where C is a calibration coefficient obtained by dividing the total reagent ion signals in laboratory calibration by the sensitivity of an amine or amide. As shown in equation (1), to minimize the effect of the variation of reagent ions during field measurements, the ambient signals of an amine or amide were normalized by the sum of ethanol clusters including protonated ethanol monomer, dimer, and trimer.

During the campaign, a Filter Inlet for Gases and AEROsols (FIGAERO) (Lopez-Hilfiker et al., 2014) was attached to the HR-ToF-CIMS. FIGAERO-HRToF-CIMS offers two operation modes. Direct gas sample analysis occurs with the HR-ToF-CIMS during simultaneous particle collection on a PTFE filter via a separate dedicated port. Particle analysis occurs via evaporation from the filter using temperature-programmed thermal desorption by heated ultra-high purity nitrogen upstream of the HR-ToF-CIMS. A moveable filter housing automatically switches between the two modes. In our

Atmos. Chem. Phys. Discuss., doi:10.5194/acp-2016-484, 2016
Manuscript under review for journal Atmos. Chem. Phys.
Published: 22 June 2016


Atmospheric Chemistry and Physics Discussions

study, measurements of ambient gaseous samples were conducted for 20 min every hour, followed by analysis of particulate samples for 40 min. In this paper, we focus on measurements of gaseous samples and present results on detection of gaseous amines and amides.

During the 20 min period for analysis of ambient gaseous samples, background measurements were auto-performed for 5 min by a motor-driven three-way Teflon solenoid valve, utilizing a high purity nitrogen flow as the background gas. Figure S4 shows typical background signals during an ambient sampling period of 3 h. The average ambient background concentrations of amines ($C_1$ to $C_6$) and amides ($C_1$ to $C_6$) throughout the field campaign are presented in Table 1. The inlet memory of amines and amides were determined using an inlet spike approach. As shown in Figure S5, the signals followed the sum of two decaying exponentials. The characteristic decaying times of two exponentials, which are displacement of amines and amides inside the inlet by pumping and removing amines and amides adsorbed on the inlet surface (Zheng et al., 2015), were 1.1 s and 8.5 s for TMA, and 1.4 s and 1.4 s for PA, respectively. These results demonstrate that a 5 min background sampling time is sufficient to eliminate the inlet memory.

All HR-ToF-CIMS data were analyzed with Tofware (Aerodyne Research, Inc. and Tofwerk AG) and Igor Pro (Wavemetrics) software. Concentrations of $O_3$ were measured by an $O_3$ analyzer (Model 49i, Thermo Scientific, USA). RH and temperature were measured by an automatic meteorological station (CAWS600, Huayun, China) at the Fudan site.

Solar radiation intensity measured by a pyranometer (Kipp & Zonen CMP6, Netherlands) was obtained from the Shanghai Pudong Environmental Monitoring Centre (31°14′ N, 121°32′ E, about 8.78 km from the Fudan site). Precipitation was recorded by a rainfall sensor (RainWise Inc., USA) located at the Huangxing Park monitoring station (31°17′ N, 121°32′ E, about 2.95 km from the Fudan site) of Shanghai Meteorology Bureau.

## 3 Results and Discussion

### 3.1 Performance of ethanol HR-ToF-CIMS in the laboratory

#### 3.1.1 Sensitivities and detection limits

The permeation rates of amines and amides were determined adopting methods of acid-base titration and hydrolysis of alkyl-amides in an acidic solution, respectively. A typical plot for

Atmos. Chem. Phys. Discuss., doi:10.5194/acp-2016-484, 2016
Manuscript under review for journal Atmos. Chem. Phys.
Published: 22 June 2016


Atmospheric Chemistry and Physics Discussions

determination of the permeation rate of the DEA permeation tube is shown in Figure S6. Plots for FA ($C_1$-amide) and PA (an isomer of $C_3$-amide) are used as examples for amides, as shown in Figure S7. In summary, at 0℃, the permeation rates of MA, DMA, TMA, and DEA permeation tubes were 6.9 ± 0.7, 7.4 ± 0.2, 5.1 ± 0.8, and 12.7 ± 0.9 ng $min^{-1}$, respectively. Permeation rates of home-made FA, AA, and PA permeation tubes were 36.7 ± 2.4, 5.2 ± 0.5, and 29.1 ± 1.6 ng $min^{-1}$, respectively, at 0℃.

The high purity nitrogen flow carrying the permeated amine/amide was then diluted with another high purity nitrogen flow at different dilution ratios, and directed to HR-ToF-CIMS for detection under dry conditions (RH = ~ 0%). Figure S8 shows the calibration curves of $C_1$- to $C_4$-amines and $C_1$- to $C_3$-amides. The derived sensitivities were 5.6-19.4 Hz $pptv^{-1}$ for amines and 3.8-38.0 Hz $pptv^{-1}$ for amides with the total reagent ions of ~0.32 MHz, respectively. Also, the detection limits of amines and amides were 0.10-0.50 pptv and 0.29-1.95 pptv at 3σ of the background signal for a 1-min integration time, respectively. Sensitivities, calibration coefficients, and detection limits of the $C_1$- to $C_4$-amines (MA, DMA, TMA, and DEA) and $C_1$- to $C_3$-amides (FA, AA, and PA), together with their proton affinities, are summarized in Table 1. The detection limits of $C_1$- to $C_3$-amines in our study are similar to those by Zheng et al. (2015) and You et al. (2014). The sensitivities of $C_1$- to $C_4$-amines are slightly better than those reported in You et al. (2014) and Yu and Lee (2012).

**3.1.2 Effects of RH and organics**

The presence of high concentrations of water is believed to have an effect on the ion-molecular reactions in IMR, given the proton transfer nature of our ion-molecular reactions and the high IMR pressure (providing longer ion-molecular reaction time) in our study. The detection of constant concentrations of amines and amides by HR-ToF-CIMS at various RH was characterized to evaluate the influence of RH. Examined were MA ($C_1$-amine) and TMA ($C_3$-amine) under 0-65% RH at 23℃, corresponding to 0-70% and 0-49% enhancement in the MS signal, respectively. In the case of amides, the increase of the PA ($C_3$-amide) signal was 0-38% under 0-55% RH. These results show that RH has an obvious effect on the MS signals for amines and amides, which followed sigmoidal fits with the $R^2 \geqslant 0.97$ in the examined RH range (Figure 1).

Figure 2 shows the effects of biogenic (α-pinene) and anthropogenic (p-xylene) compounds and their photochemical reaction products on detection of amines (MA and TMA) and amide (PA) by our HR-ToF-CIMS. After stable signals of amines/amide were established, introduction of α-pinene and

Atmos. Chem. Phys. Discuss., doi:10.5194/acp-2016-484, 2016
Manuscript under review for journal Atmos. Chem. Phys.
Published: 22 June 2016


Atmospheric Chemistry and Physics Discussions

p-xylene, respectively, had little impact on detection of amines and amides. Initiation of photochemical reactions of α-pinene and p-xylene upon turning on the Hg-lamp, as evidenced by characteristic products of pinonaldehyde from α-pinene (Lee et al., 2006) and 3-hexene-2,5-dione from p-xylene (Smith et al., 1999), respectively, did not have an obvious effect on detection of amines and amides, either.

### 3.2 Detection of amines and amides in urban Shanghai

#### 3.2.1 Identification of nitrogen-containing species

One major challenge during analysis of mass spectra from the field deployment of the ethanol HR-ToF-CIMS is to distinguish amines and amides with very close *m/z* values in order to achieve simultaneous measurements. Thanks to the high mass resolving power (R⩾3500 in V-mode) of our HR-ToF-CIMS, we are able to distinguish and identify the following protonated amines ($CH_5N{\cdot}H^+$ (*m/z* 32.0495), $C_2H_7N{\cdot}H^+$ (*m/z* 46.0651), $C_3H_9N{\cdot}H^+$ (*m/z* 60.0808), $C_4H_{11}N{\cdot}H^+$ (*m/z* 74.0964), $C_5H_{13}N{\cdot}H^+$ (*m/z* 88.1121), and $C_6H_{15}N{\cdot}H^+$ (*m/z* 102.1277)), and amides ($CH_3NO{\cdot}H^+$ (*m/z* 46.0287), $C_2H_5NO{\cdot}H^+$ (*m/z* 60.0444), $C_3H_7NO{\cdot}H^+$ (*m/z* 74.0600), $C_4H_9NO{\cdot}H^+$ (*m/z* 88.0757), $C_5H_{11}NO{\cdot}H^+$ (*m/z* 102.0913), and $C_6H_{13}NO{\cdot}H^+$ (*m/z* 116.1069)), as well as a few oxomides ($C_3H_5NO_2{\cdot}H^+$ (*m/z* 88.0393), $C_4H_7NO_2{\cdot}H^+$ (*m/z* 102.0550), and $C_5H_7NO_2{\cdot}H^+$ (*m/z* 116.0760)), as shown by the single peak fitting for each of them in Figure 3. The assignment of molecular formulas for these species is within a mass tolerance of < 10 ppm.

We further analyzed the entire mass spectra and assigned a molecular formula to 200 species with *m/z* values less than 163 Th as listed in Table S1, which allows a mass defect plot for typical 15-min mass spectra in Figure 4A. In addition to the protonated $C_1$ to $C_6$-amines and amides, their clusters with ethanol are evident, further confirming the identification of these species. A number of gaseous amines have been previously detected in the ambient air utilizing quadrupole mass spectrometer (Freshour et al., 2014; Hanson et al., 2011; Sellegri et al., 2005; You et al., 2014; Yu and Lee, 2012). As suggested by Hanson et al. (2011), an amine and an amide with one less carbon might both have high enough proton affinities and could be detected at the same unit *m/z* value by a quadrupole mass spectrometer, leading to uncertainty in measuring the ambient amine. In this study, $C_1$- to $C_6$-amines and $C_1$- to $C_6$-amides are, for the first time, systematically and simultaneously detected in ambient air.

Atmos. Chem. Phys. Discuss., doi:10.5194/acp-2016-484, 2016
Manuscript under review for journal Atmos. Chem. Phys.
Published: 22 June 2016




337 In addition to the protonated $C_1$ to $C_6$-amines and $C_1$ to $C_6$-amides and their clusters with ethanol,
338 we were able to detect many other nitrogen-containing species (*e.g.* ammonia). Among the 200
339 species with *m/z* less than 163 Th, there were 86 nitrogen-containing species (Figure 4B and Table S1).
340 Four imines (or enamines) including $CH_3N$, $C_2H_5N$, $C_3H_7N$, and $C_4H_9N$ were detected. These imines
341 (or enamines) could derive from photo-oxidation of amines (Nielsen et al., 2012). In addition, a
342 number of heterocyclic nitrogen-containing species including pyrrole, pyrroline, pyrrolidine, pyridine,
343 and pyrimidine were potentially detected (see Table S1). Apart from clusters of ammonia, $C_1$- to
344 $C_6$-amines, and $C_1$- to $C_6$-amides with water or ethanol, there were forty-eight $C_aH_bN_cO_d$ species
345 representing 55.8 % of the total nitrogen-containing species. This suggests that more than half of the
346 nitrogen-containing species existed as oxygenated compounds in the atmosphere in urban Shanghai.

347 The rest 114 species with *m/z* less than 163 Th are mostly organics (see Table S1). Above
348 *m/z*=163 Th, numerous mass peaks were observed, which are likely organics and nitrogen-containing
349 species. These high-molecular-weight species are assumed to have a low volatility and may partition
350 between the gas phase and the particles.

351 **3.2.2 Time profiles of amines and amides**

352 During the field measurement, the average RH of the diluted gaseous samples was 15.8±3.5%.
353 According to our laboratory characterization, the MS signals of MA, TMA, and PA at 15.8% RH have
354 been in average enhanced by 10%, 9%, and 19%, respectively, from our calibration under dry
355 condition. Here, we use our sigmoidal fits to convert each of our ambient data points to the signal
356 under dry condition (RH = ~0%), and calculate the corresponding concentration. Since MA and TMA
357 behaved quite similarly at elevated RH, the sigmoidal fit for TMA is also applied to the $C_2$-amines and
358 $C_4$- to $C_6$-amines. Also, the sigmoidal fit for PA is adopted for other amides. Since high purity
359 nitrogen (RH = ~0%) was used as the background sample during the ambient campaign, no
360 RH-dependent correction was made with background signals.

361 Assuming $C_1$- to $C_4$-amines have the same proton affinity as MA, DMA, TMA, and DEA,
362 respectively, the sensitivities of MA, DMA, TMA, and DEA were used to quantify $C_1$- to $C_4$-amines.
363 Since $C_5$- to $C_6$-amine standards are unavailable, the sensitivity of DEA by HR-ToF-CIMS was
364 adopted to quantify $C_5$- to $C_6$-amines. A similar approach was utilized to quantify $C_1$- to $C_3$-amides by
365 sensitivities of FA, AA, and PA, respectively. In addition, the sensitivity of PA was used to quantify

Atmos. Chem. Phys. Discuss., doi:10.5194/acp-2016-484, 2016
Manuscript under review for journal Atmos. Chem. Phys.
Published: 22 June 2016


Atmospheric Chemistry and Physics Discussions

$C_4$- to $C_6$-amides.

Figure 5 presents the time profiles for mixing ratios of $C_1$- to $C_6$-amines and $C_1$- to $C_6$-amides, respectively, from 25 July to 25 August 2015 in urban Shanghai. Note that each date point in the figure represents an average of 15-min measurements. Table 2 summarizes the mean concentrations of $C_1$- to $C_6$-amines and $C_1$- to $C_6$-amides throughout the entire campaign, together with comparison of amine and amide concentrations reported in previous field studies.

For $C_1$- to $C_6$-amines, the average concentrations (±σ) were 15.7±5.9 pptv, 40.0±14.3 pptv, 1.1±0.6 pptv, 15.4±7.9 pptv, 3.4±3.7 pptv, and 3.5±2.2 pptv, respectively. $C_1$-amine, $C_2$-amines, and $C_4$-amines were the dominant amine species in urban Shanghai. The concentrations of amines in Shanghai are generally smaller than those in Hyytiälä, Finland (Hellén et al., 2014; Kieloaho et al., 2013; Sellegri et al., 2005), potentially hinting that sources for amines existed in the forest region of Hyytiälä, Finland. Our $C_1$- and $C_2$-amines are generally more abundant than those in coastal, continental, suburban, and urban areas (Freshour et al., 2014; Hanson et al., 2011; Kieloaho et al., 2013; Sellegri et al., 2005; You et al., 2014). However, our $C_3$- to $C_6$-amines are less, potentially because we are able to distinguish an amine, an amide with one less carbon, and an oxoamide with two less carbons (see Figure 3).

For $C_1$- to $C_6$-amides, the average concentrations (±σ) were 2.3±0.7 pptv, 169.2±51.5 pptv, 778.2±899.8 pptv, 167.8±97.0 pptv, 34.5±13.3 pptv, and 13.8±5.2 pptv, respectively. $C_2$-amides, $C_3$-amides, and $C_4$-amides were the most abundant amides in urban Shanghai during the campaign and their concentrations were up to hundreds of pptv. Especially, the concentration of $C_3$-amides reached ~8700 pptv. Up to now, studies that report systematical identification and quantification of amides in the ambient air are lacking. Leach et al. (1999) detected *N*,*N*-dimethylformamide (an isomer of $C_3$-amides) of 368-4357 pptv in a suburban area surrounded by municipal incinerator, waste collection and processing center, and sewage treatment plant. In the ambient air, $C_1$- to $C_6$-amides may derive from oxidation of $C_1$- to $C_6$-amines. *N*,*N*-dimethylformamide is a major product with a yield of ~40% from photolysis experiments of TMA under high $NO_x$ conditions (Nielsen et al, 2011). Also, the yields of formamide ($C_1$-amide) and methylforamide ($C_2$-amide) from OH-initiated MA and DMA in the presence of $NO_x$ are ~11% and ~13%, respectively (Nielsen et al, 2012). Comparison of the abundance of amines and amides during the campaign, together with the yields of amides from

Atmos. Chem. Phys. Discuss., doi:10.5194/acp-2016-484, 2016
Manuscript under review for journal Atmos. Chem. Phys.
Published: 22 June 2016


Atmospheric Chemistry and Physics Discussions

photo-oxidation of amines, suggests that the ambient $C_1$- to $C_3$-amines were insufficient to explain the observed abundance of $C_1$- to $C_3$-amides. Therefore, in addition to secondary sources, $C_1$- to $C_6$-amides likely were emitted from primary sources (*e.g.* industrial emissions).

Figure 6 shows a close examination on the temporal variations of $C_2$-amines and $C_3$-amides, representatives of the observed amines and amides, together with that of rainfall between 20 August 2015 and 25 August 2015. The plots clearly reveal that the concentrations of $C_2$-amines and $C_3$-amides on raining days were much lower than those without rain, and that $C_2$-amines and $C_3$-amides rapidly went up after the rain. Previous studies reported that wet deposition is one of the important sinks of amines (Cornell et al., 2003; Ge et al., 2011a, b; You et al., 2014). Our study further indicates that wet deposition (or heterogeneous reactions) is also an important sink for amides.

**3.2.3 Diurnal patterns**

Figure 7 presents the averaged diurnal variations of $C_1$- and $C_2$-amines and $C_3$- and $C_4$-amides, together with those of temperature, radiation, and ozone concentration during the campaign. Diurnal patterns for amines and amides with less variation are exhibited in Figure S9. Mixing ratios of $C_1$- and $C_2$-amines and $C_3$- and $C_4$-amides reached their peak values in the early morning (6:00~7:00am), and then started to decline as the temperature increased. The mixing ratios were normally the lowest during the day when the temperature rose to the top. The diurnal behavior of amines and amides can be explained by the strong photochemical reactions of these species during the daytime (Barnes et al., 2010; Borduas et al., 2015; Nielsen et al., 2012), especially in summer, as evidenced by the negative correlations between the mixing ratios and radiation (exponential fits with $-0.0002 \leqslant$ exponents $\leqslant -0.0001$), and between the mixing ratios and ozone (exponential fits with $-0.003 \leqslant$ exponents $\leqslant -0.001$), a tracer for photochemical activities. Also, nighttime chemistry of amines with $NO_3$ radicals could be active. In summer night time of Shanghai, the $NO_3$ radical concentration could be up to $10^{10}$ radicals $cm^{-3}$ (Wang et al., 2013b) and the reaction rates of amines with $NO_3$ radicals are at the order of $10^{-13}$ $cm^3$ $molecular^{-1}s^{-1}$ (Nielsen et al., 2012). Hence, high mixing ratios of amines at nighttime could be a secondary source of amides through reactions of amines with $NO_3$ radicals.

In addition, an opposite tendency between the mixing ratios and the temperature (exponential fits with $-0.067 \leqslant$ exponents $\leqslant -0.049$) is clearly evident in our study, which is in contrast to the positive temperature dependence of $C_3$-amines and $C_6$-amines in previous studies (Hanson et al., 2011; You et

Atmos. Chem. Phys. Discuss., doi:10.5194/acp-2016-484, 2016
Manuscript under review for journal Atmos. Chem. Phys.
Published: 22 June 2016


Atmospheric Chemistry and Physics Discussions

al., 2014; Yu and Lee, 2012). The positive temperature dependencies of $C_3$-amines was explained by deposition of amines onto soil or grass landscape at night and then partitioning back to the atmosphere in the morning when the surface heats (Hanson et al., 2011; You et al., 2014). On the other hand, land surface in Shanghai is mainly covered by bitumen and cement, on which the behavior of amines might be different.

### 3.2.4 Source identification for $C_3$-amides

Lagrangian dispersion model has been utilized to further understand the potential sources of $C_3$-amides. This Lagrangian modeling simulation is based on Hybrid Single-Particle Lagrangian Integrated Trajectory (HYSPLIT) (Draxler and Hess, 1998; Stein et al., 2015) following the method developed by Ding et al. (2013). Three-day backward retroplumes (100 m above the ground level) from the Fudan sampling site are demonstrated for air masses with mixing ratios of $C_3$-amides > 2670 pptv in Figure 8, and for air masses with 2650 pptv > mixing ratios of $C_3$-amides > 1340 pptv in Figure S10, respectively. The embedded 12 h retroplumes give a better view of the local zones through which the air masses with high concentrations of $C_3$-amides passed before their arrival to the sampling site. Since the atmospheric lifetimes of *N*,*N*-dimethylformamide (an isomer of $C_3$-amides) and its potential precursor TMA (an isomer of $C_3$-amines) in respect to reactions with OH radicals are ~3 h and ~10 h, respectively, using an 12 h-average OH radical concentration of $2\times10^6$ radicals $cm^{-3}$, $C_3$-amides were likely emitted or formed along the trajectory. As shown in Figure 8A-D, the air plumes with high concentrations of $C_3$-amides mainly originated from the sea and came from the north of Shanghai. The air mass passed through predominantly industrial areas and cities after landing, and Baoshan industrial zone (one of the main industrial zones in Shanghai) was right on its path during the last 12 hours. Therefore, industrial emissions (or other anthropogenic emissions) might be important sources of $C_3$-amides.

Figure S10A-E presents another five cases with the next highest concentrations of $C_3$-amide. The air masses primarily came from southwest of the sampling site, and then passed through industrial areas and cities before arrival, including Songjiang and Jinshan industrial zones (another two main industrial zones in Shanghai) during the last 12 hours. These results also suggest that industrial emissions or other anthropogenic activities might be important sources of $C_3$-amides.

Atmos. Chem. Phys. Discuss., doi:10.5194/acp-2016-484, 2016
Manuscript under review for journal Atmos. Chem. Phys.
Published: 22 June 2016


Atmospheric Chemistry and Physics Discussions

## 4 Conclusions

This paper presents laboratory characterization of an ethanol HR-ToF-CIMS method for detection of amines and amides, and one month field deployment of the ethanol HR-ToF-CIMS in urban Shanghai during summer 2015. Laboratory characterization indicates that our sensitivities for amines (5.6-19.4 Hz $pptv^{-1}$) and amides (3.8-38.0 Hz $pptv^{-1}$) and detection limits for amines (0.10-0.50 pptv) and amides (0.29-1.95 pptv at 3σ of the background signal for a 1-min integration time), respectively, are slightly better than those in previous studies using CIMS methods (You et al., 2014; Yu and Lee, 2012). Correction of the mass signals of amines and amides are necessary at elevated RH because of the significant RH dependence of detection of amines and amides as observed in the laboratory. On the other hand, organics with high proton affinity are unlikely to pose an effect on the detection of amines and amides as along as their concentrations will not lead to reagent ion depletion.

High time resolution, highly sensitive and simultaneous measurements of amines (from a few pptv to hundreds of pptv) and amides (from tens of pptv to a few ppbv) have been achieved during the ambient campaign. Their diurnal profiles suggest that primary emissions could be important sources of amides in urban Shanghai, in addition to the secondary formation processes, and that photo-oxidation and wet deposition of amines and amides might be their main loss pathway.

86 nitrogen-containing species including amines and amides were identified with *m/z* less than 163 Th, 55.8% of which are oxygenated. This certainly indicates that the ethanol HR-ToF-CIMS method potentially has a much wider implication in terms of measuring atmospheric nitrogen-containing species. For example, imines (or enamines) and a number of heterocyclic nitrogen-containing compounds (*e.g.* pyridine and quinoline) (see Table S1) were potentially detected by this method. Berndt et al. (2014) reported that pyridine was able to enhance nucleation in $H_2SO_4/H_2O$ system. Also, proton affinities of most of these heterocyclic nitrogen-containing compounds are higher than that of ammonia, hence they potentially have the capacity to neutralize atmospheric acidic species (*e.g.* $H_2SO_4$, $HNO_3$ and organic acids) to contribute to secondary particle formation and growth.

Nevertheless, the detection of amides in ambient air is consistent with the photochemical chemistry that has been previously studied in the laboratory (Nielsen et al, 2012). Compared with amines, acetamide has a very weak positive enhancement on nucleation capability of sulfuric acid

Atmos. Chem. Phys. Discuss., doi:10.5194/acp-2016-484, 2016
Manuscript under review for journal Atmos. Chem. Phys.
Published: 22 June 2016


Atmospheric Chemistry and Physics Discussions

(Glasoe et al., 2015). On the other hand, the mixing ratios of amides were significantly higher than those of amines in urban Shanghai during our measurements. Since the newly formed nano-particles are likely highly acidic (Wang et al., 2010a), hydrolysis of amides will give rise to $NH_4^+$ in the particle, in addition to those formed through direct neutralization between gaseous ammonia and particulate sulfuric acid. Although significant progresses on the roles of ammonia and amines in the atmospheric nucleation have been made (Almeida et al., 2013; Kürten et al., 2014) and it has been shown that acetamide can only slightly enhance the nucleation rate of sulfuric acid (Glasoe et al., 2015), the exact contribution of amides during atmospheric nucleation and subsequent growth events is yet to be elucidated.

## Acknowledgement

This study was financially supported by the National Natural Science Foundation of China (No. 21190053, 21222703, 21561130150, & 41575113), the Ministry of Science & Technology of China (2012YQ220113-4), and the Cyrus Tang Foundation (No. CTF-FD2014001). LW thanks the Royal Society-Newton Advanced Fellowship (NA140106).

Atmos. Chem. Phys. Discuss., doi:10.5194/acp-2016-484, 2016
Manuscript under review for journal Atmos. Chem. Phys.
Published: 22 June 2016


Atmospheric Chemistry and Physics Discussions

## References

Almeida, J., Schobesberger, S., Kürten, A., Ortega, I. K., Kupiainen-Määttä, O., Praplan, A. P., Adamov, A., Amorim, A., Bianchi, F., Breitenlechner, M., David, A., Dommen, J., Donahue, N. M., Downard, A., Dunne, E., Duplissy, J., Ehrhart, S., Flagan, R. C., Franchin, A., Guida, R., Hakala, J., Hansel, A., Heinritzi, M., Henschel, H., Jokinen, T., Junninen, H., Kajos, M., Kangasluoma, J., Keskinen, H., Kupc, A., Kurtén, T., Kvashin, A. N., Laaksonen, A., Lehtipalo, K., Leiminger, M., Leppä, J., Loukonen, V., Makhmutov, V., Mathot, S., McGrath, M. J., Nieminen, T., Olenius, T., Onnela, A., Petäjä, T., Riccobono, F., Riipinen, I., Rissanen, M., Rondo, L., Ruuskanen, T., Santos, F. D., Sarnela, N., Schallhart, S., Schnitzhofer, R., Seinfeld, J. H., Simon, M., Sipilä, M., Stozhkov, Y., Stratmann, F., Tome, A., Tröstl, J., Tsagkogeorgas, G., Vaattovaara, P., Viisanen, Y., Virtanen, A., Vrtala, A., Wagner, P. E., Weingartner, E., Wex, H., Williamson, C., Wimmer, D., Ye, P., Yli-Juuti, T., Carslaw, K. S., Kulmala, M., Curtius, J., Baltensperger, U., Worsnop, D. R., Vehkamäki, H., and Kirkby, J.: Molecular understanding of sulphuric acid-amine particle nucleation in the atmosphere, Nature, 502, 359-363, 10.1038/nature12663, 2013.

Barnes, I., Solignac, G., Mellouki, A., and Becker, K. H.: Aspects of the Atmospheric Chemistry of Amides, ChemPhysChem, 11, 3844-3857, 10.1002/cphc.201000374, 2010.

Barsanti, K. C., and Pankow, J. F.: Thermodynamics of the formation of atmospheric organic particulate matter by accretion reactions - Part 3: Carboxylic and dicarboxylic acids, Atmos. Environ., 40, 6676-6686, 10.1016/j.atmosenv.2006.03.013 ,2006.

Bertram, T. H., Kimmel, J. R., Crisp, T. A., Ryder, O. S., Yatavelli, R. L. N., Thornton, J. A., Cubison, M. J., Gonin, M., and Worsnop, D. R.: A field-deployable, chemical ionization time-of-flight mass spectrometer, Atmos.Meas.Tech., 4, 1471-1479, 10.5194/amt-4-1471-2011, 2011.

Berndt, T., Sipilä, M., Stratmann, F., Petäjä, T., Vanhanen, J., Mikkilä, J., Patokoski, J., Taipale, R., Mauldin III, R. L., and Kulmala, M.: Enhancement of atmospheric $H_2SO_4/H_2O$ nucleation: organic oxidation products versus amines, Atmos. Chem. Phys., 14, 751–764, 10.5194/acp-14-751-2014, 2014.

Borduas, N., da Silva, G., Murphy, J. G., and Abbatt, J. P.: Experimental and theoretical understanding of the gas phase oxidation of atmospheric amides with OH radicals: kinetics, products, and mechanisms, J. Phys.Chem. A, 119, 4298-4308, 10.1021/jp503759f, 2015.

Bunkan, A. J. C., Mikoviny, T., Nielsen, C. J., and Wisthaler, A.: Experimental and theoretical study of the OH-initiated photo-oxidation of formamide, J. Phys.Chem. A, 120, 1222-1230, 10.1021/acs.jpca.6b00032, 2016.

Cornell, S. E., Jickells, T. D., Cape, J. N., Rowland, A. P., and Duce, R. A.:Organics nitrogen deposition on land and coastal environments: a review od methods and data, Atmos. Environ., 37, 2173-2191, 10.1016/S1352-2310(03)00133-X, 2003.

Cox, R. A., and Yates, K.: The hydrolyses of benzamides, methylbenzimidatium ions, and lactams in aqueous sulfuric-acid - the excess acidity method in the determination of reaction-mechanisms, Can. J. Chem., 59, 2853-2863, Doi 10.1139/V81-414, 1981.

Draxler, R.R., and Hess,G.D.: An overview of the HYSPLIT_4 modeling system of trajectories, dispersion, and deposition. Aust. Meteor. Mag., 47, 295-308,1998.

Ding, A. J., Wang, T., and Fu, C. B.: Transport characteristics and origins of carbon monoxide and ozone in Hong Kong, South China, J. Geophys. Res. Atmos., 118, 9475-9488, 10.1002/jgrd.50714, 2013.

El Dib, G., and Chakir, A.: Temperature-dependence study of the gas-phase reactions of atmospheric NO3 radicals with a series of amides, Atmos. Environ., 41, 5887-5896, 10.1016/j.atmosenv.2007.03.038, 2007.

Erupe, M. E., Viggiano, A. A., and Lee, S. H.: The effect of trimethylamine on atmospheric nucleation involving $H_2SO_4$, Atmos. Chem. Phys., 11, 4767-4775, 10.5194/acp-11-4767-2011, 2011.



542 Finlayson-Pitts, B. J., and Pitts, J. N.: Chemistry of the upper and lower atmosphere : theory, experiments, and
543 applications, Academic Press, San Diego, xxii, 969 p. pp., 2000.
544 Freshour, N. A., Carlson, K. K., Melka, Y. A., Hinz, S., Panta, B., and Hanson, D. R.: Amine permeation sources
545 characterized with acid neutralization and sensitivities of an amine mass spectrometer, Atmos. Meas. Tech.,
546 7, 3611-3621, 10.5194/amt-7-3611-2014, 2014.
547 Glasoe, W. A., Volz, K., Panta, B., Freshour, N., Bachman, R., Hanson, D. R., McMurry, P. H., and Jen.C.:
548 Sulfuric acid nucleation : an experimental study of the effect of seven bases, J. Geophys. Res. Atmos., 120,
549 1933-1950, 10.1002/2014JD022730, 2015.
550 Ge, X., Wexler, A. S., and Clegg, S. L.: Atmospheric amines – Part I. A review, Atmos. Environ., 45, 524-546,
551 10.1016/j.atmosenv.2010.10.012, 2011.
552 Hanson, D. R., McMurry, P. H., Jiang, J., Tanner, D., and Huey, L. G.: Ambient Pressure Proton Transfer Mass
553 Spectrometry: Detection of Amines and Ammonia, Environ. Sci. Technol., 45, 8881-8888,
554 10.1021/es201819a, 2011.
555 Hellén, H., Kieloaho, A. J., and Hakola, H.: Gas-phase alkyl amines in urban air; comparison with a boreal
556 forest site and importance for local atmospheric chemistry, Atmos. Environ., 94, 192-197,
557 10.1016/j.atmosenv.2014.05.029, 2014.
558 Kieloaho, A.-J., Hellén, H., Hakola, H., Manninen, H. E., Nieminen, T., Kulmala, M., and Pihlatie, M.:
559 Gas-phase alkylamines in a boreal Scots pine forest air, Atmos. Environ., 80, 369-377,
560 10.1016/j.atmosenv.2013.08.019, 2013.
561 Kim, H. A., Kim, K., Heo, Y., Lee, S. H., and Choi, H. C.: Biological monitoring of workers exposed to
562 N,N-dimethylformamide in synthetic leather manufacturing factories in Korea, Int. Arch. Occup. Environ.
563 Health, 77, 108-112, 10.1007/s00420-003-0474-1, 2004.
564 Kuhn, U., Sintermann, J., Spirig, C., Jocher, M., Ammann, C., and Neftel, A.: Basic biogenic aerosol precursors:
565 Agricultural source attribution of volatile amines revised, Geophys. Res. Lett., 38, L16811,
566 doi:10.1029/2011GL047958 , 2011.
567 Kürten, A., Jokinen, T., Simon, M., Sipilä, M., Sarnela, N., Junninen, H., Adamov, A., Almeida, J., Amorim, A.,
568 Bianchi, F., Breitenlechner, M., Dommen, J., Donahue, N. M., Duplissy, J., Ehrhart, S., Flagan, R. C.,
569 Franchin, A., Hakala, J., Hansel, A., Heinritzi, M., Hutterli, M., Kangasluoma, J., Kirkby, J., Laaksonen, A.,
570 Lehtipalo, K., Leiminger, M., Makhmutov, V., Mathot, S., Onnela, A., Petäjä, T., Praplan, A. P., Riccobono,
571 F., Rissanen, M. P., Rondo, L., Schobesberger, S., Seinfeld, J. H., Steiner, G., Tomé, A., Tröstl, J., Winkler,
572 P. M., Williamson, C., Wimmer, D., Ye, P., Baltensperger, U., Carslaw, K. S., Kulmala, M., Worsnop, D. R.,
573 and Curtius, J.: Neutral molecular cluster formation of sulfuric acid-dimethylamine observed in real time
574 under atmospheric conditions, Proc.Natl.Acad.Sci., 111, 15019-15024, 10.1073/pnas.1404853111, 2014.
575 Leach, J., Blanch, A., and Bianchi, A. C.: Volatile organic compounds in an urban airborne environment adjacent
576 to a municipal incinerator, waste collection centre and sewage treatment plant, Atmos. Environ., 33,
577 4309-4325, Doi 10.1016/S1352-2310(99)00115-6, 1999.
578 Lee, A., Goldstein, A. H., Kroll, J. H., Ng, N. L., Varutbangkul, V., Flagan, R. C., and Seinfeld, J. H.: Gas-phase
579 products and secondary aerosol yields from the photooxidation of 16 different terpenes, J. Geophys. Res.
580 Atmos., 111, Artn D1730510.1029/2006jd007050, 2006.
581 Lee, D., and Wexler, A. S.: Atmospheric amines – Part III: Photochemistry and toxicity, Atmos. Environ., 71,
582 95-103, 10.1016/j.atmosenv.2013.01.058, 2013.
583 Lopez-Hilfiker, F. D., Mohr, C., Ehn, M., Rubach, F., Kleist, E., Wildt, J., Mentel, T. F., Lutz, A., Hallquist, M.,
584 Worsnop, D., and Thornton, J. A.: A novel method for online analysis of gas and particle composition:
585 description and evaluation of a Filter Inlet for Gases and AEROsols (FIGAERO), Atmos.Meas.Tech., 7,



983-1001, 10.5194/amt-7-983-2014, 2014.

Ma, Y., Xu, X., Song, W., Geng, F., and Wang, L.: Seasonal and diurnal variations of particulate organosulfates in urban Shanghai, China, Atmos. Environ., 85, 152-160, 10.1016/j.atmosenv.2013.12.017, 2014.

Malloy, Q. G. J., Qi, L., Warren, B., Cocker, D. R., Erupe, M. E., and Silva, P. J.: Secondary organic aerosol formation from primary aliphatic amines with $NO_3$ radical, Atmos. Chem. Phys., 9, 2051-2060, 2009.

Murphy, S. M., Sorooshian, A., Kroll, J. H., Ng, N. L., Chhabra, P., Tong, C., Surratt, J. D., Knipping, E., Flagan, R. C., and Seinfeld, J. H.: Secondary aerosol formation from atmospheric reactions of aliphatic amines, Atmos. Chem. Phys.,7, 2313-2337, 2007.

Nielsen, C. J., Herrmann, H., and Weller, C.: Atmospheric chemistry and environmental impact of the use of amines in carbon capture and storage (CCS), Chem. Soc. Rev., 41, 6684-6704, 10.1039/c2cs35059a, 2012.

Nielsen, C. J., D'Anna, B., Karl, M., Aursnes, M., Boreave, A.,Bossi, R., Bunkan, A. J. C., Glasius, M., Hallquist, M., Hansen,A.-M. K., Kristensen, K., Mikoviny, T., Maguta, M. M., Müller,M., Nguyen, Q., Westerlund, J., Salo, K., Skov, H., Stenstrøm, Y.,and Wisthaler, A.: Atmospheric Degradation of Amines (ADA), Norwegian Institute for Air Research, Kjeller, Norway, 2011.

Nowak, J. B.: Chemical ionization mass spectrometry technique for detection of dimethylsulfoxide and ammonia, J. Geophys. Res. Atmos., 107, 10.1029/2001jd001058, 2002.

NIST: NIST Standard Reference Database Number 69, edited, National Institute for Standard Technology (NIST) Chemistry Web Book, available at: http://webbook.nist.gov/chemistry/ (last access: 23 May 2016), 2016.

Qiu, C., Wang, L., Lal, V., Khalizov, A. F., and Zhang, R.: Heterogeneous reactions of alkylamines with ammonium sulfate and ammonium bisulfate, Environ. Sci. Technol., 45, 4748-4755, 10.1021/es1043112, 2011.

Sellegri, K., Hanke, M., Umann, B., Arnold, F., and Kulmala, M.: Measurements of organic gases during aerosol formation events in the boreal forest atmosphere during QUEST, Atmos. Chem. Phys., 5, 373-384, 2005.

Smith, D. F., Kleindienst, T. E., and McIver, C. D.: Primary product distributions from the reaction of OH with m-, p-xylene, 1,2,4- and1,3,5-trimethylbenzene,J.Atmos.Chem.,34,339-364,Doi10.1023/A:1006277328628, 1999.

Smith, J. N., Barsanti, K. C., Friedli, H. R., Ehn, M., Kulmala, M., Collins, D. R., Scheckman, J. H., Williams, B. J., and McMurry, P. H.: Observations of aminium salts in atmospheric nanoparticles and possible climatic implications, Proc.Natl.Acad.Sci., 107, 6634-6639, 10.1073/pnas.0912127107, 2010.

Stein, A.F., Draxler, R.R, Rolph, G.D., Stunder, B.J.B., Cohen, M.D., and Ngan, F.: NOAA's HYSPLIT atmospheric transport and dispersion modeling system, B. Am. Meteorol. Soc., 96, 2059-2077, doi:10.1175/BAMS-D-14-00110.1, 2015.

VandenBoer, T. C., Petroff, A., Markovic, M. Z., and Murphy, J. G.: Size distribution of alkyl amines in continental particulate matter and their online detection in the gas and particle phase, Atmos. Chem. Phys., 11, 4319–4332, 10.5194/acp-11-4319-2011, 2011.

Wang, L., Khalizov, A. F., Zheng, J., Xu, W., Ma, Y., Lal, V., and Zhang, R.: Atmospheric nanoparticles formed from heterogeneous reactions of organics, Nat. Geosci., 3, 238-242, 10.1038/ngeo778, 2010a.

Wang, L., Lal, V., Khalizov, A. F., and Zhang, R. Y.: Heterogeneous Chemistry of Alkylamines with Sulfuric Acid: Implications for Atmospheric Formation of Alkylaminium Sulfates, Environ. Sci. Technol., 44, 2461-2465, 10.1021/es9036868, 2010b.

Wang, L., Du, H., Chen, J., Zhang, M., Huang, X., Tan, H., Kong, L., and Geng, F.: Consecutive transport of anthropogenic air masses and dust storm plume: Two case events at Shanghai, China, Atmos. Res., 127, 22-33, 10.1016/j.atmosres.2013.02.011, 2013a.

Wang, S., Shi, C., Zhou, B., Zhao, H., Wang, Z., Yang, S., and Chen, L.: Observation of NO3 radicals over



630 Shanghai, China, Atmos. Environ., 70, 401-409, 10.1016/j.atmosenv.2013.01.022, 2013b.
631 Wang, X. K., Rossignol, S., Ma, Y., Yao, L., Wang, M. Y., Chen, J. M., George, C., and Wang, L.: Molecular
632 characterization of atmospheric particulate organosulfates in three megacities at the middle and lower
633 reaches of the Yangtze River, Atmos. Chem. Phys., 16, 2285-2298, 10.5194/acp-16-2285-2016, 2016.
634 Xiao, S., Wang, M. Y., Yao, L., Kulmala, M., Zhou, B., Yang, X., Chen, J. M., Wang, D. F., Fu, Q. Y., Worsnop,
635 D. R., and Wang, L.: Strong atmospheric new particle formation in winter in urban Shanghai, China, Atmos.
636 Chem. Phys.,15, 1769-1781, 10.5194/acp-15-1769-2015, 2015.
637 You, Y., Kanawade, V. P., de Gouw, J. A., Guenther, A. B., Madronich, S., Sierra-Hernández, M. R., Lawler, M.,
638 Smith, J. N., Takahama, S., Ruggeri, G., Koss, A., Olson, K., Baumann, K., Weber, R. J., Nenes, A., Guo,
639 H., Edgerton, E. S., Porcelli, L., Brune, W. H., Goldstein, A. H., and Lee, S. H.: Atmospheric amines and
640 ammonia measured with a chemical ionization mass spectrometer (CIMS), Atmos. Chem. Phys., 14,
641 12181-12194, 10.5194/acp-14-12181-2014, 2014.
642 Yu, H., and Lee, S.-H.: Chemical ionisation mass spectrometry for the measurement of atmospheric amines,
643 Environ. Chem., 9, 190, 10.1071/en12020, 2012.
644 Yu, H., McGraw, R., and Lee, S. H.: Effects of amines on formation of sub-3 nm particles and their subsequent
645 growth, Geophys. Res. Lett., 39, Artn L0280710.1029/2011gl050099, 2012.
646 Zhang, R., Khalizov, A., Wang, L., Hu, M., and Xu, W.: Nucleation and growth of nanoparticles in the
647 atmosphere, Chem. Rev., 112, 1957-2011, 10.1021/cr2001756, 2012.
648 Zheng, J., Ma, Y., Chen, M., Zhang, Q., Wang, L., Khalizov, A. F., Yao, L., Wang, Z., Wang, X., and Chen, L.:
649 Measurement of atmospheric amines and ammonia using the high resolution time-of-flight chemical
650 ionization mass spectrometry, Atmos. Environ., 102, 249-259, 10.1016/j.atmosenv.2014.12.002, 2015.
651 Zhu, L., Schade, G. W., and Nielsen, C. J.: Real-time monitoring of emissions from monoethanolamine-based
652 industrial scale carbon capture facilities, Environ. Sci. Technol., 47, 14306-14314, 10.1021/es4035045,
653 2013.
654

Atmos. Chem. Phys. Discuss., doi:10.5194/acp-2016-484, 2016
Manuscript under review for journal Atmos. Chem. Phys.
Published: 22 June 2016


Table 1. Proton affinity, sensitivity, calibration coefficient, 1-min detection limit at 3σ of background signal during the laboratory characterization, and ambient background of selected amines and amides.

| Compounds | Proton affinity (kcal $mol^{-1}$) (NIST, 2016) | Sensitivity (mean ± σ) (Hz $pptv^{-1}$)[a] | Calibration coefficient ($10^{-2}$ MHz $Hz^{-1}$ pptv) | Detection limit (pptv) | Ambient background (mean ± σ) (pptv)[b] |
|---|---|---|---|---|---|
| Water | 165.2 | | | | |
| Ethanol | 185.6 | | | | |
| Ammonia | 204.0 | | | | |
| Methylamine ($C_1$-amine) | 214.9 | 7.06 ± 0.2 | 4.67 | 0.23 | 3.88 ± 1.23 |
| Dimethylamine (an isomer of $C_2$-amines) | 222.2 | 5.6 ± 0.2 | 5.89 | 0.50 | 6.64 ± 1.24 |
| Trimethylamine (an isomer of $C_3$-amines) | 226.8 | 19.4 ± 1.3 | 1.70 | 0.10 | 0.41 ± 0.14 |
| Diethylamine (an isomer of $C_4$-amines) | 227.6 | 6.4 ± 0.4 | 5.03 | 0.42 | 3.59 ± 1.04 |
| *N*,*N*-dimethyl-2-propanamine (an isomer of $C_5$-amines) | 232.0 | | | | 0.68 ± 0.32 |
| Triethylamine (an isomer of $C_6$-amines) | 234.7 | | | | 1.76 ± 0.79 |
| Formamide (an isomer of $C_1$-amide) | 196.5 | 38.0 ± 1.2 | 0.78 | 0.29 | 0.59 ± 0.50 |
| Acetamide (an isomer of $C_2$-amides) | 206.4 | 3.8 ± 0.3 | 7.89 | 0.45 | 8.63 ± 3.63 |
| *N*-methylformamide (an isomer of $C_2$-amides) | 203.5 | | | | |
| Propanamide (an isomer of $C_3$-amides) | 209.4 | 4.4 ± 0.1 | 6.82 | 1.95 | |
| *N*-methylacetamide (an isomer of $C_3$-amides) | 212.4 | | | | 59.76 ± 48.37 |
| *N*,*N*-dimethylformamide (an isomer of $C_3$-amides) | 212.1 | | | | |
| *N*-ethylacetamide (an isomer of $C_4$-amides) | 214.6 | | | | 13.59 ± 10.01 |
| *N*,*N*-dimethylacetamide ( an isomer of $C_4$-amides) | 217.0 | | | | |
| *2*,*2*-dimethyl-propanamide ( an isomer of $C_5$-amides) | 212.5 | | | | 8.47 ± 5.18 |
| *N*,*N*-dimethyabutyramide ( an isomer of $C_6$-amides) | 220.3 | | | | 2.60 ± 1.40 |

[a] Sensitivities were obtained under total reagent ion signals of ~ 0.32 MHz;

[b] Mean background values throughout the entire campaign ± one standard deviation for $C_1$-to $C_6$-amines and $C_1$-to $C_6$-amides.

Atmos. Chem. Phys. Discuss., doi:10.5194/acp-2016-484, 2016
Manuscript under review for journal Atmos. Chem. Phys.
Published: 22 June 2016


660 Table 2 Inter-comparison of gaseous amines and amides measured in different locations with different surroundings.
661

| Location (site type, season) | $C_1$-Amine (pptv) | $C_2$-Amines (pptv) | $C_3$-Amines (pptv) | $C_4$-Amines (pptv) | $C_5$-Amines (pptv) | $C_6$-Amines (pptv) | $C_1$-Amide (pptv) | $C_2$-Amides (pptv) | $C_3$-Amides (pptv) | $C_4$-Amides (pptv) | $C_5$-Amides (pptv) | $C_6$-Amides (pptv) | Ref. |
|---|---|---|---|---|---|---|---|---|---|---|---|---|---|
| Hyytiälä, Finland (Forested, Spring) | | 12.2±7.7[a] | 59±35.5[a] | | | | | | | | | | Sellegri et al.(2005) |
| Hyytiälä, Finland (Forested,Summer and Autumn) | | 157±20[b] | 102±61[b] | 15.5±0.5[b] | | | | | | | | | Kieloaho et al.(2013) |
| Hyytiälä, Finland (Forested,Summer) | | 39.1[c] | 10.2[c] | 8.1[c] | | 1.6[c] | | | | | | | Hellén et al.(2014) |
| Alabama, USA (Forested,Summer) | < 1.2 | < 4.8 | 1-10 | < 23.1 | < 17.3 | < 13.0 | | | | | | | You et al. (2014) |
| Kent, USA (Suburban,Winter) | < 18 | 8 ± 3[a] | 16 ± 7[a] | < 41 | | < 8 | | | | | | | Yu and Lee. (2012) |
| Kent, USA (Suburban,Summer) | 1-4 | < 4.4 | 5-10 | 10-50 | 10-100 | < 13.1 | | | | | | | You et al. (2014) |
| Southampton, UK (Suburban,Spring,Summer and Autumn) | | | | | | | | | 368-4357 | | | | Leach et al.(1999) |
| Lewes, USA (Coastal,Summer） | 5[c] | 28[c] | 6[c] | 3[c] | 1[c] | 2[c] | | | | | | | Freshour et al. (2014) |
| Lamont, USA (Continental,Spring) | 4[c] | 14[c] | 35[c] | 150[c] | 98[c] | 20[c] | | | | | | | Freshour et al. (2014) |
| Nanjing, China (Industrialized,Summer) | 0.1-18.9 | 0.1-29.9 | 0.1-9.3 | | | | | | | | | | Zheng et al. (2014) |
| Atlanta, USA (Urban,Summer) | < 0.2 | 0.5-2 | 4-15 | ~5[d] | 4-5[d] | 3-25 | | | | | | | Hanson et al. (2011) |
| Helsinki, Finland (Urban,Summer) | | 23.6[c] | 8.4[c] | 0.3[c] | | 0.1[c] | | | | | | | Hellén et al.(2014) |
| Toroton, Canada (Urban,Summer) | | < 2.7 | | < 2.7 | | < 1.0 | | | | | | | VandenBoer et al.(2011) |
| Shanghai, China (Urban,Summer) | 15.7±5.9[e] | 40.0±14.3[e] | 1.1±0.6[e] | 15.4±7.9[e] | 3.4±3.7[e] | 3.5±2.2[e] | 2.3±0.7[e] | 169.2±51.5[e] | 778.2±899.8[e] | 167.8±97.0[e] | 34.5±13.3[e] | 13.8±5.2[e] | This study |

662 [a] Mean values ± one standard deviation;
663 [b] The highest concentrations during the measurement;
664 [c] Mean values;
665 [d] 8 h average values;
666 [e] Mean values throughout the entire campaign ± one standard deviation.

Atmos. Chem. Phys. Discuss., doi:10.5194/acp-2016-484, 2016
Manuscript under review for journal Atmos. Chem. Phys.
Published: 22 June 2016


Atmospheric Chemistry and Physics Discussions

667 **Figure captions:**
668
669 **Figure 1.** Influences of RH on the MS signals of methylamine (MA), trimethylamine (TMA), and
670 propanamide (PA).
671
672 **Figure 2.** Influences of organics on MS signals of methylamine (MA, panels A and B),
673 trimethylamine (TMA, panels A and B), and propanamide (PA, panels C and D). Note that the right
674 axis is used for the signal with an identical color, and other signals correspond to the left axis.
675
676 **Figure 3.** High-resolution single peak fitting for amines and amides.
677
678 **Figure 4.** Mass defect diagram for (A) protonated amines ($C_1$-$C_6$) and amides ($C_1$-$C_6$) and their
679 clusters with ethanol, together with other species with *m/z* less than 163 Th in the ambient sample;
680 and (B) all nitrogen-containing species with *m/z* less than 163 Th in the ambient sample. Circle
681 diameters are proportional to $\log_{10}$(count rates).
682
683 **Figure 5.** Time series of amines (panel A) and amides (panel B). Concentrations of amines and
684 amides are 15-min average values.
685
686 **Figure 6.** Time profiles of the rainfall, $C_2$-amines and $C_3$-amides.
687
688 **Figure 7.** The averaged diurnal profiles of $C_1$- and $C_2$-amines and $C_3$- and $C_4$-amides, together with
689 those of temperature, radiation, and ozone concentration during the campaign.
690
691 **Figure 8.** Three-day backward retroplumes (100 m above the ground level) from the sampling
692 location at (**A**) 05:00, 12 August 2015; (**B**) 21:00, 20 August 2015; (**C**) 06:00, 21 August 2015; and (**D**)
693 06:00, 25 August 2015. The embedded boxes show 12 h backward trajectories.
694
695
696
697
698
699
700
701
702
703
704
705
706
707
708
709

Atmos. Chem. Phys. Discuss., doi:10.5194/acp-2016-484, 2016
Manuscript under review for journal Atmos. Chem. Phys.
Published: 22 June 2016


Atmospheric Chemistry and Physics Discussions

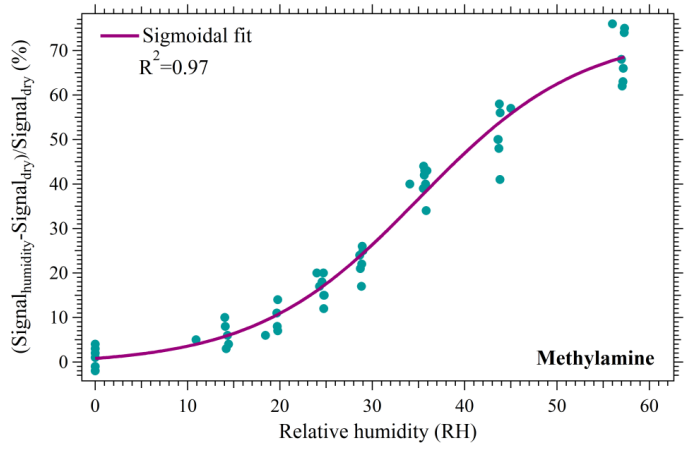


710

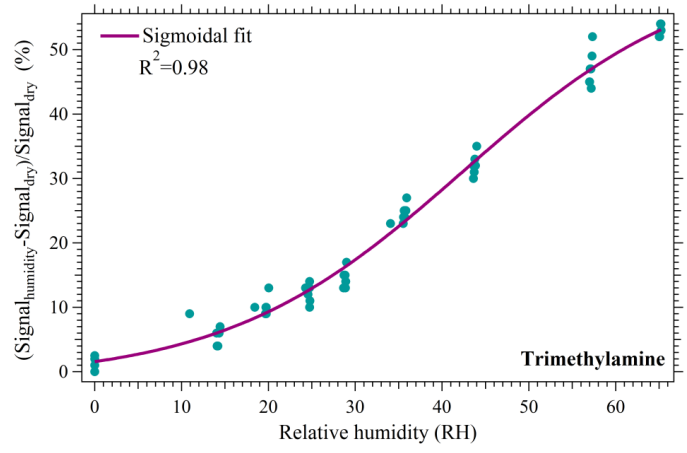


711

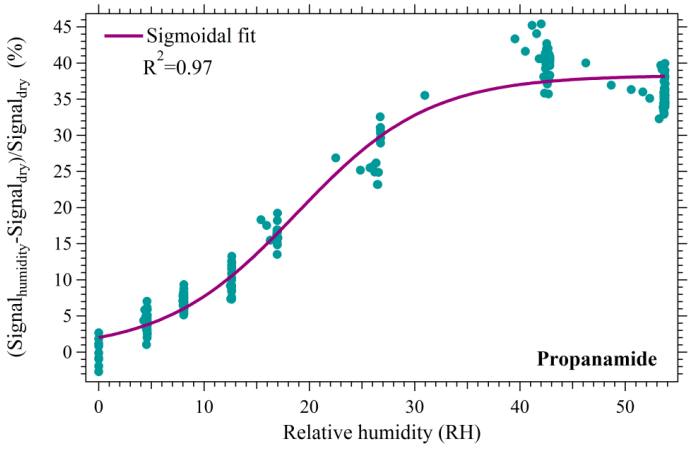


712

713

714 **Figure 1**

Atmos. Chem. Phys. Discuss., doi:10.5194/acp-2016-484, 2016
Manuscript under review for journal Atmos. Chem. Phys.
Published: 22 June 2016


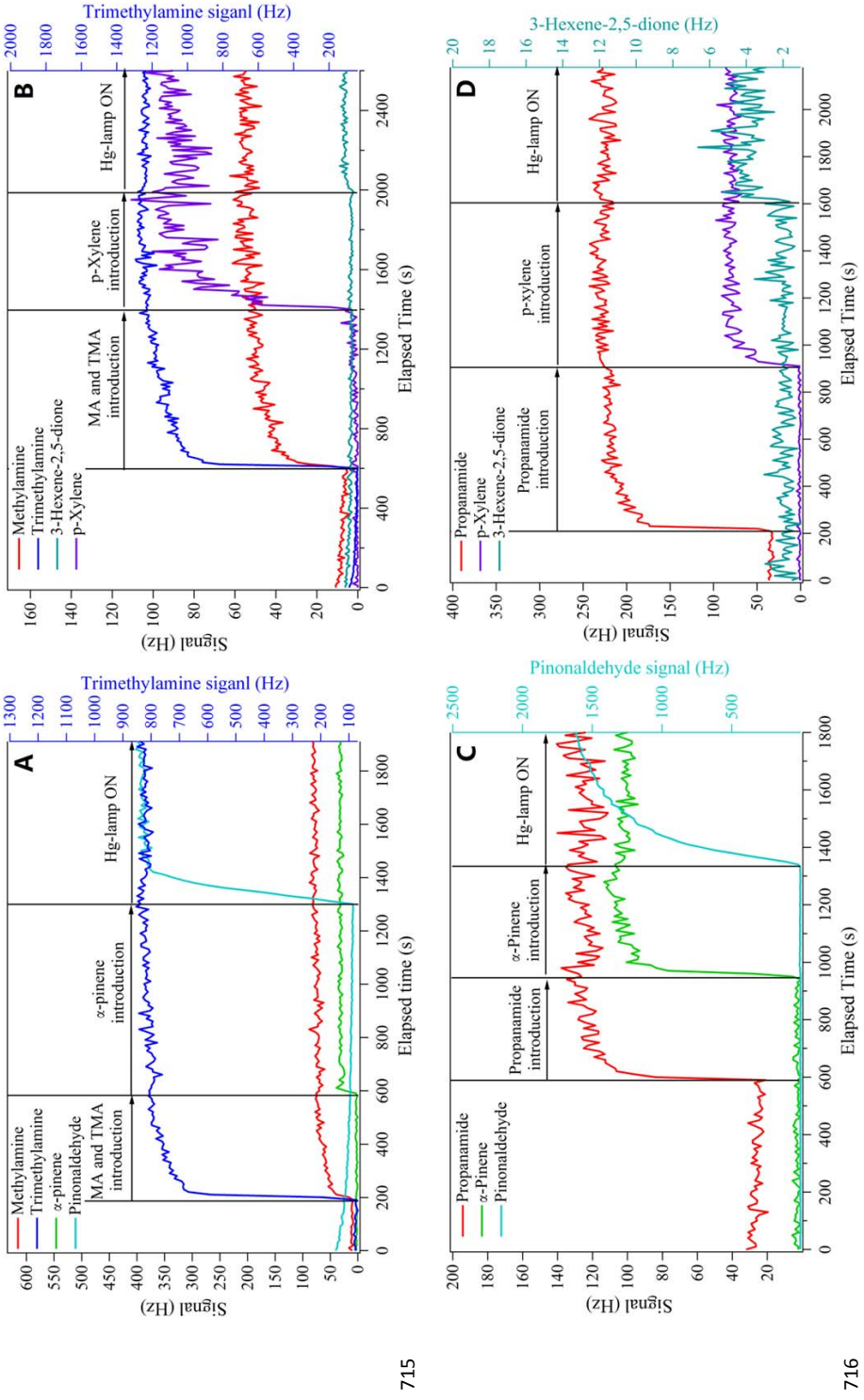


**Figure 2**

Atmos. Chem. Phys. Discuss., doi:10.5194/acp-2016-484, 2016
Manuscript under review for journal Atmos. Chem. Phys.
Published: 22 June 2016


Atmospheric Chemistry and Physics Discussions

718
719
720
721
722
723
724
725

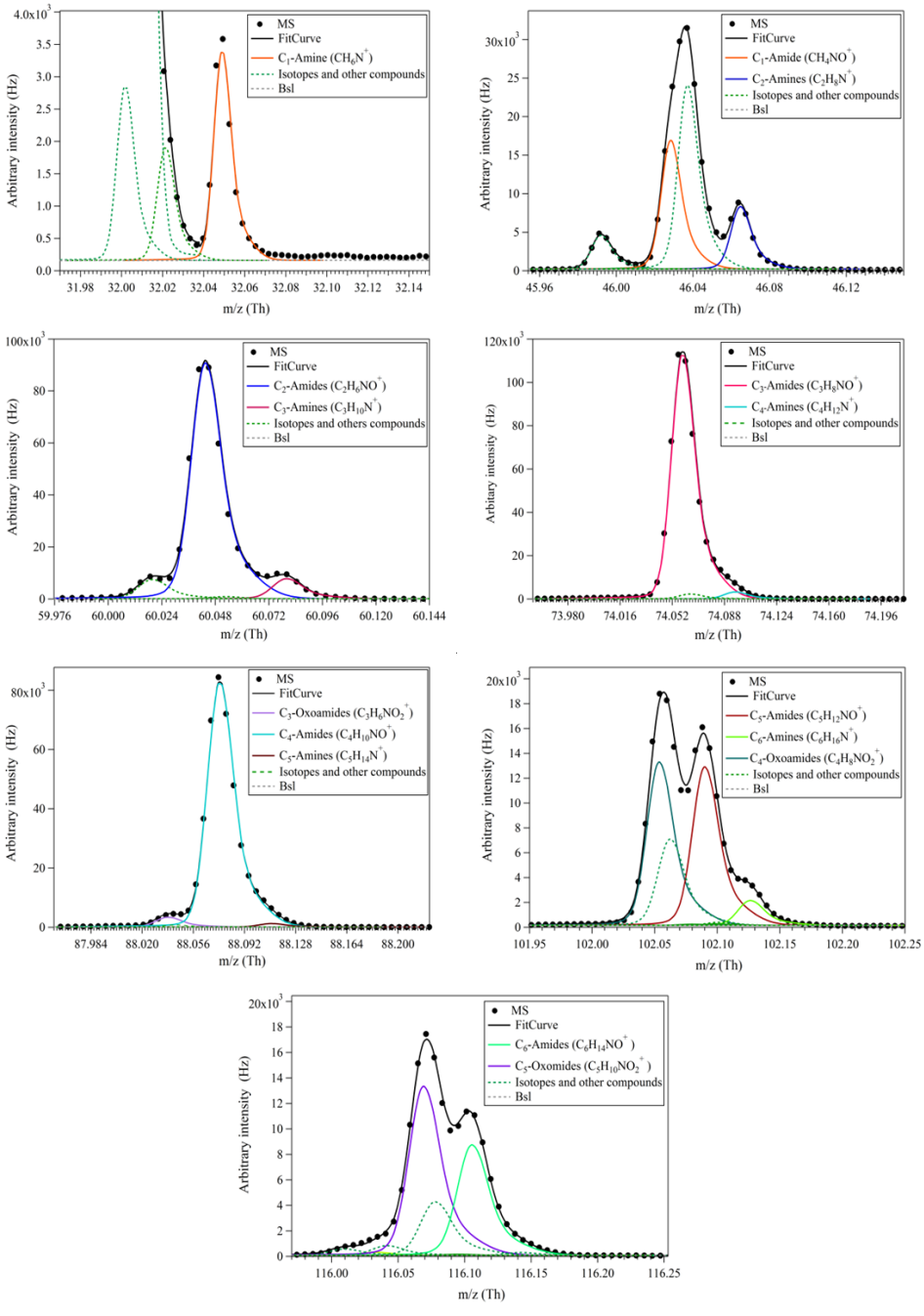


**Figure 3**

Atmos. Chem. Phys. Discuss., doi:10.5194/acp-2016-484, 2016
Manuscript under review for journal Atmos. Chem. Phys.
Published: 22 June 2016


Atmospheric Chemistry and Physics Discussions

726

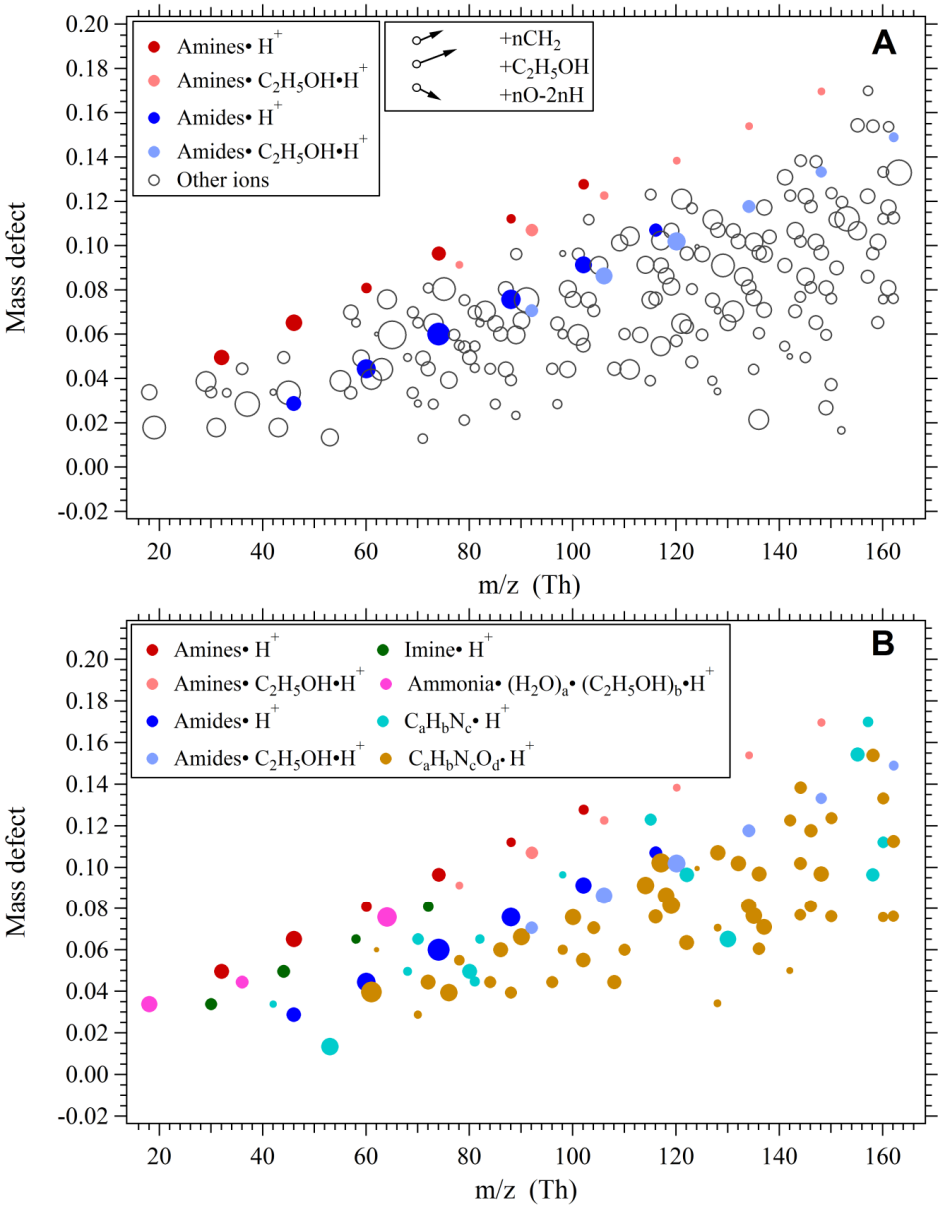


727

728 **Figure 4**

729

Atmos. Chem. Phys. Discuss., doi:10.5194/acp-2016-484, 2016
Manuscript under review for journal Atmos. Chem. Phys.
Published: 22 June 2016


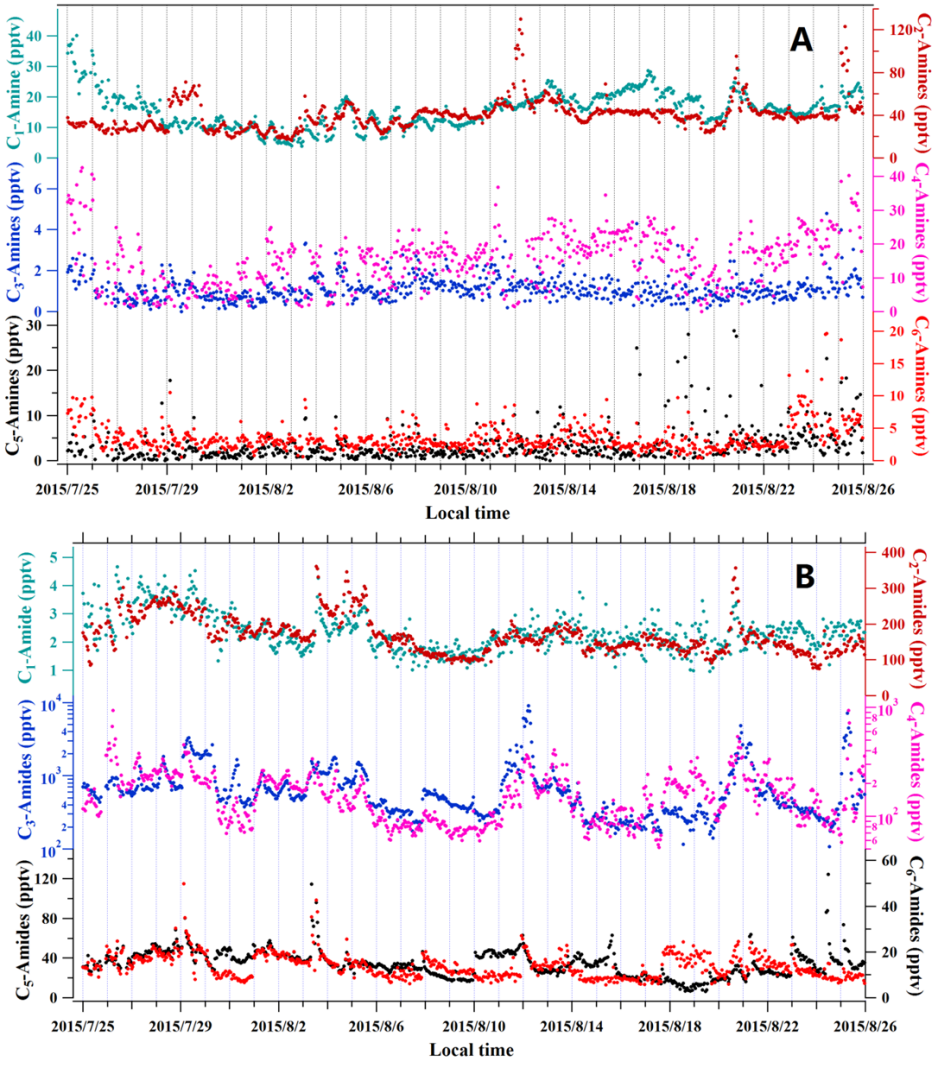


**Figure 5**

Atmos. Chem. Phys. Discuss., doi:10.5194/acp-2016-484, 2016
Manuscript under review for journal Atmos. Chem. Phys.
Published: 22 June 2016


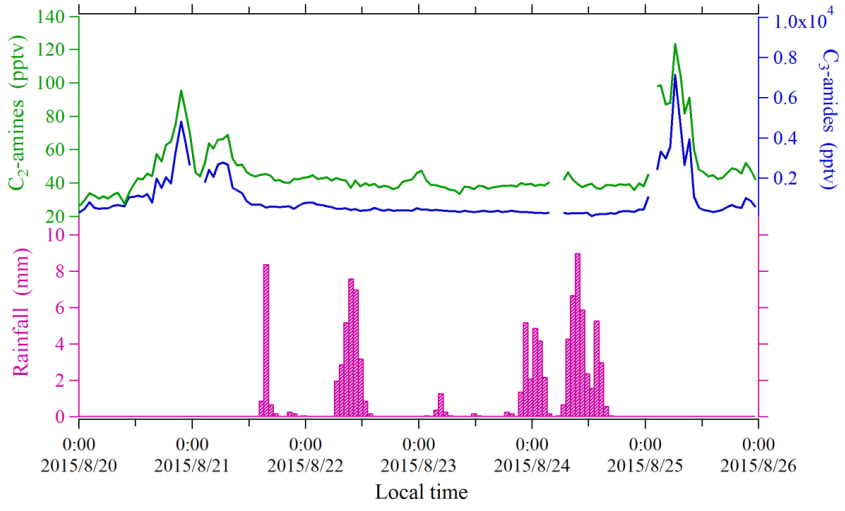


**Figure 6**

Atmos. Chem. Phys. Discuss., doi:10.5194/acp-2016-484, 2016
Manuscript under review for journal Atmos. Chem. Phys.
Published: 22 June 2016


Atmospheric Chemistry and Physics Discussions

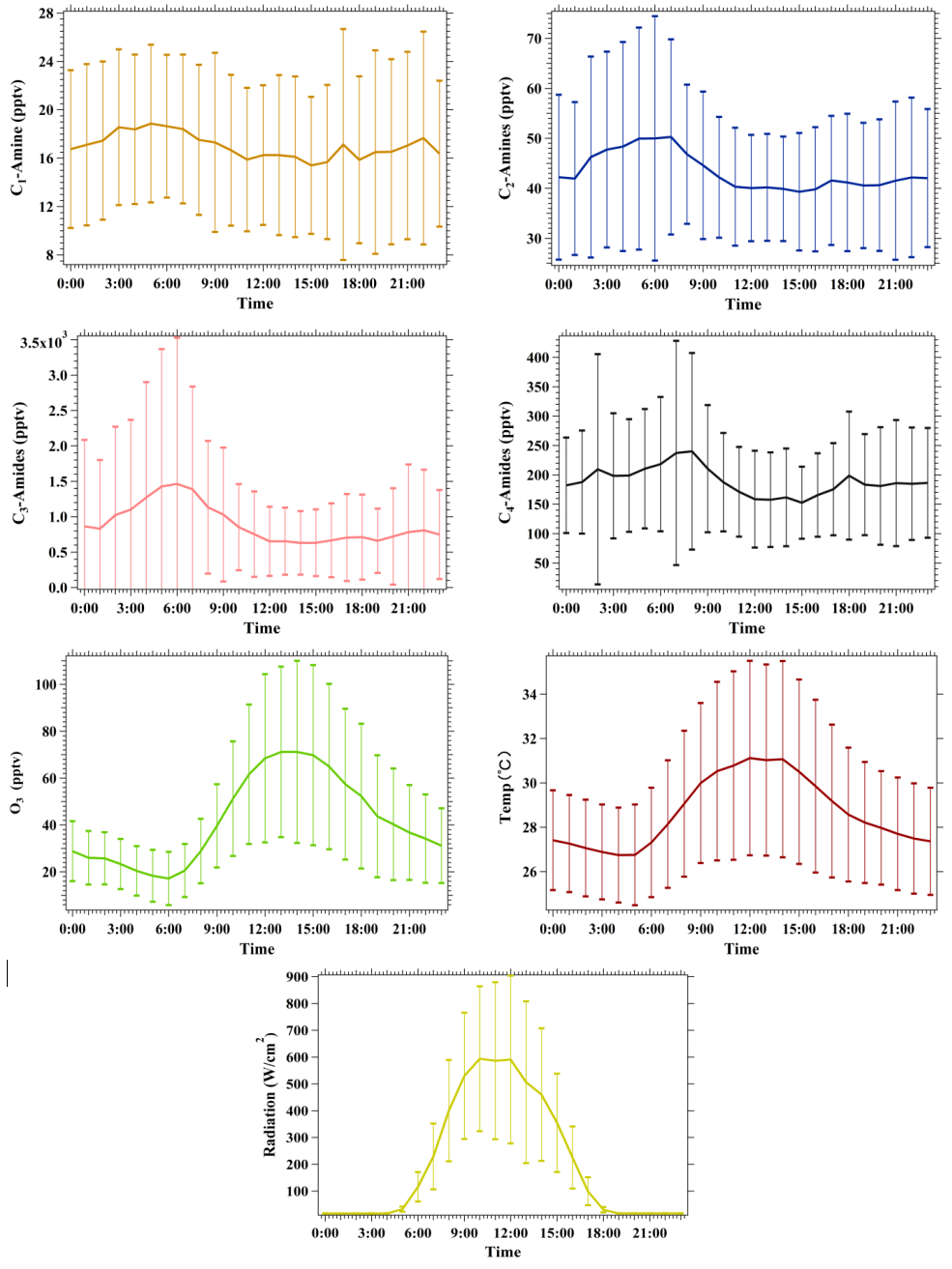


**Figure 7**

Atmos. Chem. Phys. Discuss., doi:10.5194/acp-2016-484, 2016
Manuscript under review for journal Atmos. Chem. Phys.
Published: 22 June 2016


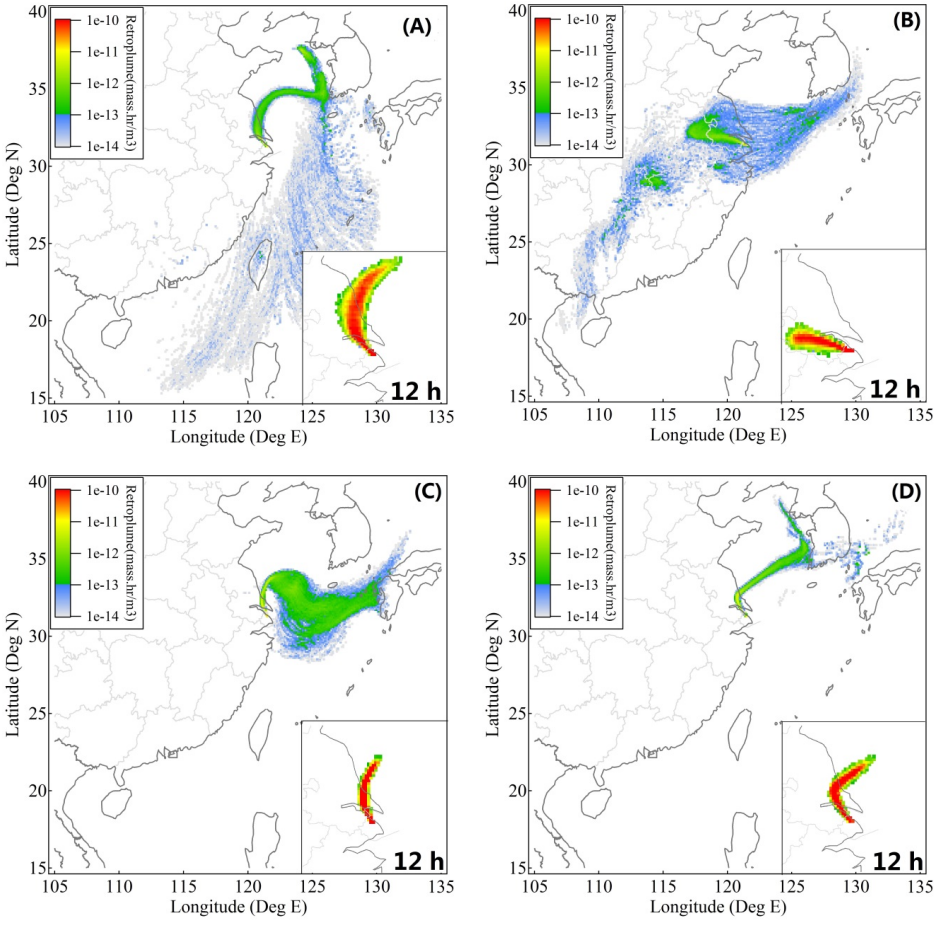


**Figure 8**